

Journal of Materials Chemistry C

Accepted Manuscript



This is an *Accepted Manuscript*, which has been through the Royal Society of Chemistry peer review process and has been accepted for publication.

Accepted Manuscripts are published online shortly after acceptance, before technical editing, formatting and proof reading. Using this free service, authors can make their results available to the community, in citable form, before we publish the edited article. We will replace this *Accepted Manuscript* with the edited and formatted *Advance Article* as soon as it is available.

You can find more information about *Accepted Manuscripts* in the [Information for Authors](#).

Please note that technical editing may introduce minor changes to the text and/or graphics, which may alter content. The journal's standard [Terms & Conditions](#) and the [Ethical guidelines](#) still apply. In no event shall the Royal Society of Chemistry be held responsible for any errors or omissions in this *Accepted Manuscript* or any consequences arising from the use of any information it contains.

ARTICLE

Phosphorescent oxygen sensors produced by spot-crazing of polyphenylenesulfide films

Cite this: DOI: 10.1039/x0xx00000x

Claudio Toncelli^a, Olga V. Arzhakova^b, Alla Dolgova^b, Aleksandr L. Volynskii^b, Joseph P. Kerry^c, Dmitri B. Papkovsky^{a,*}

Received 00th January 2014,
Accepted 00th January 2014

DOI:

www.rsc.org/

Phosphorescent oxygen sensors based on PtBP and PdBP dyes encapsulated in polyphenylenesulfide (PPS) films by spot-crazing method are described. The new polymer matrix enables simple, one-step production of discrete, high-performance O₂ sensors using a low toxicity solvent 2-butanone, low overall strain (8 %), low amounts solvent and precise spatial control. The resulting nano-structured sensor materials display markedly enhanced brightness, high photo, mechanical and chemical stability. Their structural and physico-chemical properties were characterized by differential scanning calorimetry (DSC), wide-angle X-ray scattering (WAXS), optical microscopy and phosphorescence lifetime imaging microscopy (PLIM). The PPS sensors show high degree of lateral and in-depth homogeneity on micro and macro-scale, as revealed by confocal microscopy, linear Stern-Volmer plots and single-exponential decays. Operating in phosphorescence lifetime mode, optimised sensors show stable O₂ calibrations in the range 0.1-100 kPa O₂, low temperature dependence (linear in the range 10-50°C), low cross-sensitivity to humidity and high reproducibility (RSD 1.5% at 21 kPa and 0.5% at zero O₂). This technology facilitates the production of low-cost disposable O₂ sensors and their integration in large scale industrial applications such as packaging.

Introduction

Detection of molecular oxygen (O₂) by a non-chemical, reversible, contactless optical method¹ is of high utility for many areas including industrial process control, environmental monitoring, biological detection, medicine and food packaging.²⁻⁴ Solid-state phosphorescence based O₂-sensitive materials satisfy these requirements, unlike the other technologies such as Clark-type electrodes.³ Optical sensors are usually produced by encapsulation of an O₂-sensitive indicator dye in an O₂-permeable, mechanically and chemically stable quenching medium such as polymers or other matrices (e.g. glass fibres, membranes).⁵ The characteristics of the dye and encapsulation/quenching medium determine the sensitivity and other operational characteristics of the resulting sensor material.⁶ Selection of the quenching medium is based on the nature and physico-chemical properties of the dye, fabrication process requirements and application specifications. It normally comprises common polymers such as polystyrene (PS), silicones, ormosils, fluorinated polymers^{3, 7-8}, with physically entrapped (solid solution) or covalently bound dye molecules⁹ prepared in the form of a thin film coating or composite. Often such sensors contain an additional support to improve the mechanical properties of the film and aid handling, incorporation into the sample and optical measurements.¹⁰ Conventional O₂ sensors are usually produced by making a

polymeric cocktail in an organic solvent, applying it on a substrate and drying,¹¹ polymerizing or curing liquid precursors.¹² These processes usually involve toxic solvents or monomers (e.g. styrene), in significant amount and with considerable wastage. Solvent crazing of polymers in physically active liquid environments (PALEs) allows encapsulation of various thermodynamically incompatible additives in polymeric substrates.^{17,18-19} This approach involves tensile drawing of a polymer film or a fibre in a suitable solvent containing a dissolved additive which leads to the development of a specific nanoporous structure in the polymer (5–15nm pores with a narrow size distribution, and volume porosity up to 55-60 %). This process is controlled by the nature of the polymer (chemical structure, degree of crystallinity, organization of crystalline phase for semi-crystalline polymers), PALE, deformation conditions (tensile strain, applied stress, strain rate, temperature) and the concentration of an incorporated additive in the feed solution.²⁰ This technique has been applied to encapsulate phosphorescent O₂-sensitive dyes in high-density polyethylene (HDPE) and polypropylene films in a spot-method which considerably reduces the amount of solvent used (toluene).²¹ However, intensity signals, temperature stability and mechanical properties of such sensors are not as good as for traditional sensors. Also after solvent-crazing these materials require additional washing and annealing steps. Polyphenylenesulfide (PPS) is an attractive polymer for sensor development due to its high chemical and thermal (up to 240°C)

stability, negligible swelling in solvents and water uptake, moderate O₂ permeability^{13,14}. As an engineering thermoplastic, PPS films have excellent mechanical properties even without reinforcement, they are used in aerospace industry and heavy duty composites. It can potentially be used for O₂ sensing at high temperatures.¹⁵⁻¹⁶ However, rigid aromatic backbone, insolubility in organic solvents, extrusion at high temperatures and poor processability make PPS hard to impregnate with O₂ sensitive dyes and produce O₂ sensors.

We hypothesised that extruded PPS films possess the required characteristics (moderate elongation at break, ductile behaviour and chemical resistance) for the use in the solvent-crazing process and fabrication of high-performance O₂ sensors. Using sheets of commercial PPS film, phosphorescent dyes PtBP and PdBP, and 2-butanone as a low toxicity solvent, we optimized the production of discrete O₂ sensors by the local spot-crazing process with a precise spatial control. We also studied key physico-chemical, spectroscopic and O₂ sensing characteristics of the PPS sensors showing their superiority over existing sensors.

Experimental

Materials. Fortron® films (blown PPS, 75 μm thick) were from CSHyde (Netherlands). Pt(II)- and Pd(II) complexes of meso-tetrabenzoporphyrin (PtBP and PdBP)- from Frontier Scientific (USA). Analytical grade 2-butanone, ethyl acetate, toluene, anisole, dimethylsulfoxide and glacial acetic acid were from Sigma-Aldrich. O₂ and N₂ gases, 99.9% were from Irish Oxygen (Ireland).

Spot-crazing procedure. A strip of PPS film (3.0 x 5.0 cm) was clamped in a custom-made drawing device¹⁸ and 10 μL of PtBP solution (0.1-0.4 mg/ml) in the appropriate solvent were applied with a micropipette to the centre of the film, which was then immediately stretched at a constant strain rate of 6 mm min⁻¹ to the desired tensile strain (4-12% elongation). The film was then wiped to remove residual solvent, dried in air and released. The process is shown schematically in Fig. 1.

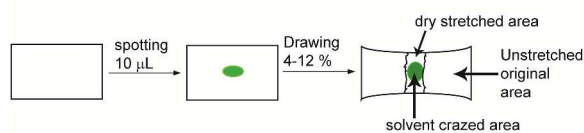


Figure 1. Scheme of spot-crazing of PPS films in 2-butanone and fabrication of discrete O₂ sensors.

Spectroscopic and structural characterisation of PPS samples.

Phosphorescence intensity and lifetime signals from PPS sensors were measured with a hand-held instrument OptechTM (Mocon, USA): three times in different locations and calculating average values and standard deviations. O₂ calibrations were performed using a phase detector FirestingTM (PyroSciences, Germany) operating with a 1 mm optical fibre probe. Phase shift readings were converted into lifetime values as follows: $\tau = \tan(\theta) / (2 \cdot \pi \cdot \vartheta)$, where τ is the lifetime (μs), θ - phase shift (rad), and ϑ - modulation frequency (4.0 kHz). Accuracy of lifetime measurements using Optech and Firesting instruments was 0.01 μs. Phosphorescence

decays were measured on a Cary Eclipse spectrophotometer (Varian) using total gate time 1 ms, gate time 0.05 ms, number of flashes 10, and delay time 0.1 ms for PdBP and 0.02 for PtBP, and lifetime calculation from single-exponential fitting.

Standard O₂/N₂ gas mixtures (0-100kPa O₂) produced by a precision gas mixer (LN Industries, Switzerland) were pumped through a flow cell containing a sensor which was interrogated with the FirestingTM probe. The flow cell consisted of an air tight metal frame with a glass lens for optical detection, submerged in a circulating water bath (Julabo, Germany) and connected to calibration gases with PEEK tubing. Humidity effects were tested by flushing the sensors with standard gas mixtures bubbled through a humidifier bottle half-filled with water. Photostability was assessed by exposing the sensor to continuous excitation on the FirestingTM device, for 8.5 h at maximal (100%) LED power.

The DSC scans of PPS samples (~1.0 mg each) were collected on a thermal analyser Netzsch DSC 204 Phoenix (Germany), at a heating rate 20°C/min. The device was calibrated with an indium reference sample. The wide-angle X-ray scattering diffractograms were recorded on a DRON-4 diffractometer (Bourestnik, Russia, CuK_α-irradiation, wavelength $\lambda = 0.154$ nm). Morphology of the spot-crazed PPS films was studied on a METAM-2 polarised light microscope (LOMO, Russia). Confocal fluorescence microscopy was performed on a TCSPC-PLIM system (Becker&Hickl, Germany) based on an upright microscope Axio Examiner Z1 (Zeiss, Germany) with oil immersion objective Neofluar 100x/1.3, heated stage with motorized Z-axis control, DCS-120 confocal scanner (B&H) with two excitation and two emission channels.²² A 405 nm picosecond diode laser (B&H), connected to the DCS-120 scanner with an optical fibre was used for the excitation. Emission was detected with a 750-810 nm bandpass filter and R10467U-40 photon counting detector (Hamamatsu) connected to the scanner and controlled by TCSPC hardware.²³

Results and discussion

Fabrication and initial testing of PPS based O₂ sensors. Unlike HDPE and PP films which can be stretched by more than 200% in air and solvent-crazed in different solvents²¹, PPS films possess a low elongation at break (<50%¹⁴) and their behaviour during crazing in different solvents is largely unknown. We examined the feasibility of spot-crazing of PPS films in several solvent systems which also dissolve PtBP: toluene, anisole, ethyl acetate and acetic acid. Unfortunately, all these were deemed unusable as they increased brittleness of the film causing its fracture at low tensile strains (<1%) without any significant staining of the polymer. The only suitable solvent was 2-butanone, which provided stable crazing of PPS films with total elongation of up to 12% and efficient staining with PtBP. Notably, upon tensile drawing only part of the polymer which was covered with 2-butanone underwent significant deformation (Fig. 1). Increasing PtBP concentration increased phosphorescence intensity signals from the sensors, though not in a linear manner. 0.1-0.2 mg/ml of PtBP produced bright intensity signals, while at >0.4 mg/ml precipitation of the dye on the surface started to occur. On the other hand, phosphorescence lifetime signals from the spots remained stable, but the unquenched lifetime, τ_0 , in PPS was reduced

by 4–8 μs compared to the PS or HDPE sensors (Table 1). The % of total and local elongation of the PPS was seen to have marginal effect on intensity and lifetime signals. The low impact of the main process parameters on sensor characteristics reflects the robustness of the fabrication method. Low tensile strains required for PPS are beneficial, as this speeds up the process, facilitates spatial control and preserves the shape of the substrate. O_2 permeability of bulk PPS is ~ 9 times lower than for PS (11.8 vs 102.4 $\text{cm}^3\text{mm}/\text{m}^2\text{day.atm}$, at 23 °C¹⁴). Nonetheless, solvent-crazed PPS-PtBP sensors showed only ~ 2 -fold lower quenchability than conventional PtBP-PS sensors (33% and 59% at 21 kPa O_2 – Table 1). As a result, PPS-PtBP sensors allow measurement up to 100 kPa O_2 , which is useful e.g. for food packaging. For comparison, conventional PS sensors can become inaccurate at above 50 kPa O_2 ²⁴. To cope with reduced sensitivity of the PPS sensors in 0–2 kPa O_2 range, PtBP dye can be substituted with PdBP which has a longer lifetime (see below).

We also found that the PPS sensors do not require additional post-treatments, producing stable and reproducible sensing characteristics straight after fabrication. In contrast, HDPE and PP based solvent-crazed sensors require annealing at elevated temperature and washing with organic solvent²¹.

Thus, the low toxicity solvent 2-butanone (class 3 according to ICH guide²⁶) and spot-crazing with small drops of dye solution have enabled simple and bio-sustainable fabrication of discrete O_2 sensors from extruded PPS films. Such sensors show bright phosphorescent signals, stable and reproducible lifetime signals comparable with conventional microporous sensors and much higher than solvent-crazed HDPE sensors²¹. Optimised (*vide supra*) PPS-PtBP sensors then underwent a detailed characterization.

Table 1. The characteristics of PPS-PtBP sensors produced by spot-crazing in 2-butanone under different conditions.

Parameter	Specification	I_0 (zero kPa O_2) (FU)	I_q (21 kPa O_2) (FU)	τ_0 (zero kPa O_2) (μs)	τ_q (21 kPa O_2) (μs)
Concentration (mg/ml)	0.1	4300 \pm 600	3400 \pm 350	44.88 \pm 0.35	31.00 \pm 1.04
	0.2	6200 \pm 900	4350 \pm 500	44.73 \pm 0.19	30.91 \pm 0.94
	0.3	8050 \pm 500	4950 \pm 1150	44.37 \pm 0.14	29.88 \pm 0.97
	0.4	8500\pm700	5500\pm1050	44.61\pm0.44	29.57\pm0.57
Elongation (%)	3.8 ^a (70 ^b)	9250 \pm 850	5900 \pm 250	44.60 \pm 0.12	29.45 \pm 0.32
	7.9^a(120^b)	11200\pm1100	7000\pm450	44.81\pm0.26	29.64\pm0.94
	7.9 ^a (185 ^b)	8900 \pm 2300	5850 \pm 1150	45.04 \pm 0.14	29.72 \pm 0.08
	12.4 ^a (210 ^b)	6200 \pm 750	4400 \pm 400	44.00 \pm 0.69	29.46 \pm 1.33
PtBP-HDPE sensor (annealed, measured on a white support)	n/a ²⁵	9100 \pm 1300 ^b	2200 \pm 200 ^b	48.45 \pm 0.06	13.13 \pm 0.17
PtBP-PS coating on a microporous support	n/a	14000 \pm 2100 ^b	4700 \pm 300 ^b	51.99 \pm 0.10	21.15 \pm 0.09

I and τ represent sensor intensity and lifetime signals, respectively, measured with OptechTM at 24 °C. Optimal conditions are in bold.

a - total elongation; b - elongation within the crazed section. Unless specified otherwise, sensors were made from 75- μm thick PPS using 10 μl of dye solution 0.40 mg/ml, total elongation 8 %.

Physicochemical and structural characterisation. PPS is by nature a crystallisable polymer, hence part of it exists in the crystalline state and the rest in the amorphous (disordered) state^{27–28}. To characterize its crystalline structure, the original PPS film was analysed by DSC and wide-angle X-ray scattering (WAXS). DSC allows the estimation of thermal characteristics of polymers, including glass transition temperature, melting temperature and degree of crystallinity^{27–28}. The scan in **Fig 2A** shows the temperature interval which includes the glass transition of the non-crystalline fraction, the cold crystallization and melting temperature intervals. Glass transition temperature was seen to be 91.2 °C, meaning that at room temperature the amorphous phase of the PPS exists in its glassy state. A pronounced peak at 124 °C is associated with cold crystallization of the amorphous part of PPS. Finally, the polymer melts at 279 °C. To estimate the overall crystallinity of initial PPS, the area under the melting peak (29.11 J/g) was corrected for the area under the crystallization peak (25.44 J/g) giving a value of 3.67 J/g, which should then be normalized for the heat of fusion of 100% crystalline PPS. Although the latter parameter is not available, its

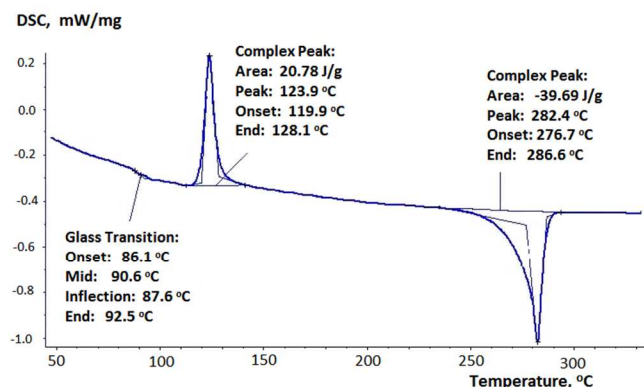
indirect estimates range from 80 J/g^{27, 29} to 150 J/g³⁰. Thus, the crystallinity of initial PPS is estimated to be less than 4%.

Unlike DSC, WAXS measures crystallinity directly. Diffraction pattern in **Fig 2B** shows a small Bragg peak at $2\theta = 12.5^\circ$ also indicating that crystallinity of PPS is below 10%³¹. Hence, PPS is essentially amorphous polymer in its glassy state with minor inclusions of crystallites. Its behaviour upon deformation in PALE is expected to follow the classical solvent crazing of glassy amorphous polymers³², being substantially different from the highly crystalline (64%) HDPE with rubbery amorphous phase²⁵.

The above conclusion was confirmed by the analysis of solvent-crazed PPS samples by optical microscopy (**Fig 3**). One can see that deformation of PPS in 2-butanone proceeds via nucleation and growth of crazes and formation of a typical fibrillar-porous structure. The crazes nucleate at the surface defects in the polymer, then the craze tip advances perpendicularly to the direction of the applied stress (Fig. 3A) and, at higher tensile strains, the crazes widen and move their walls apart (Fig. 3B). This is accompanied by a transition of the polymer from non-oriented to the oriented state in craze fibrils. Dye molecules dissolved in PALE penetrate the structure of

sub-micron crazes and fill them up. After solvent evaporation, dye molecules are trapped and adsorbed on the surface of nanofibrils, visualising the crazes in uniform green colour.

A



B

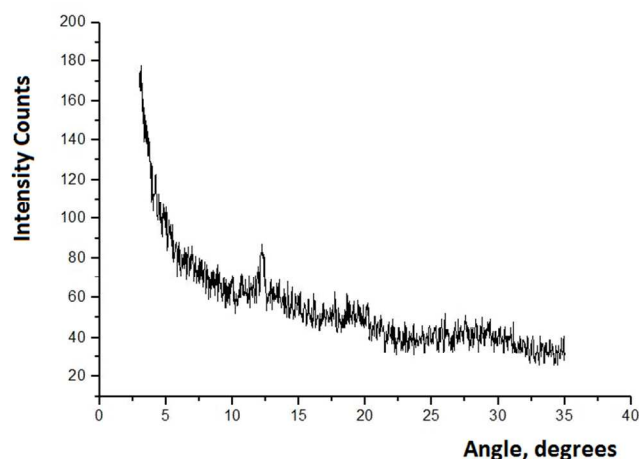


Fig. 2. Physico-chemical characterisation of the PPS sensors by DSC scan (A) and WAXS diffractogram (B). The inset in DSC graph shows the glass transition temperature.

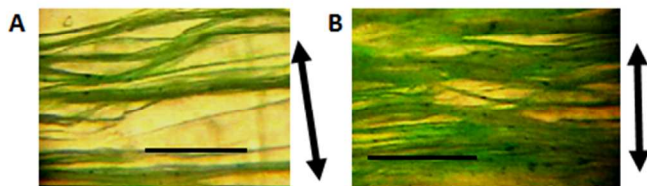


Fig. 3. Optical micrographs of the PPS samples after tensile strain (direction is shown by arrows) by 15% (A) and 40% (B) in dye-containing 2-butanone. The scale bar is 1 mm.

By measuring changes in the geometrical volume upon elongation, the porosity of the solvent-crazed PPS samples was estimated to be: 4–5% at 10% strain, 7–8% at 20% strain and 12% at 40% strain.

In summary, deformation of PPS in 2-butanone proceeds via classical solvent crazing mechanism, with nucleation and growth of numerous crazes with their typical fibrillar-porous structure. The dye solution rapidly penetrates the formed structure by stress-induced

hydrodynamic flow and occupies the volume of crazes. After solvent evaporation, dye molecules remain trapped in the web-like structure of crazes, producing highly phosphorescent O₂-sensitive material. So far, the use of solvent crazing in O₂ sensing was demonstrated only with semi-crystalline polymers (HDPE and PP - two papers by our group). With PPS a glassy polymer was used for the first time in solvent-crazing to produce O₂ sensors, and this was shown to follow classical crazing mechanism. This knowledge can be applied to other glassy polymers and sensor materials.

Sensor operational performance. Full calibrations of PtBP-PPS sensors were carried out over 0–100 kPa O₂ and 10–50 °C temperature ranges (Fig. 4). Similar to the solvent-crazed HDPE sensors²¹, good linearity of Stern-Volmer plots for average lifetimes was observed (e.g. R² = 0.996 at 10 °C, Fig. 4A), which allows simple recalibration. As expected, at higher temperatures, quenching was higher (Fig. 4D). For the studied range (10–50 °C), it followed a linear dependence (though general case is described by a more complex function³³). Temperature cross-sensitivity of PPS sensors in this range was 0.5–0.8%/K, which is lower than for PS sensors (1–1.5%/K at 21 kPa and 100 kPa O₂^{3,34}). Comparison of calibrations in the gas and liquid phase revealed that PPS sensors possess practically no cross-sensitivity to humidity: 1.3% at 10 °C and 2.0% at 30 °C. This is in line with the high hydrophobicity, rigidity, minimal swelling and water uptake by PPS¹⁴ - the criteria reported for other O₂ sensors³⁵. For different sensors from the same batch, the RSD were 1.5% at 21 kPa and 0.5% at zero O₂ (N=4). The limit of detection (LOD) of 0.47 kPa corresponds to the variation of lifetime signal of 0.26 μs at 0 kPa O₂, 10 °C.

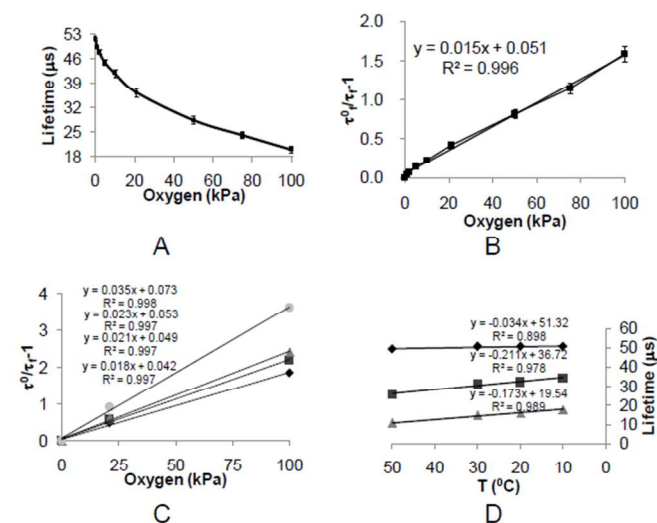


Figure 4. Calibrations of PtBP-PPS sensors in the gas phase (N=3). **A.** Lifetime calibration at 10 °C; **B.** Stern-Volmer plots for A. **C.** Stern-Volmer plots at 10 (♦), 20 (■), 30 (▲) and 50 °C (●). **D.** Temperature dependence of lifetime at different pO₂. Measured with Firesting™ instrument.

While operating reliably over 0.5–100 kPa O₂ range, the sensitivity of PtBP-PPS sensors at around zero O₂ is less than for PS or HDPE based sensors²¹. This can be tuned by substituting PtBP with another dye with longer lifetime or O₂ quenchability³⁴. Using the same

procedure, we produced PPS sensors from PdBP dye and compared them with PtBP sensors. Phosphorescence decays measured on Cary Eclipse spectrometer were single-exponential and clearly different for the two dyes at two O₂ points (Fig. 5A,B). This also reflects uniform distribution and quenchability of dye molecules in solvent-crazed PPS, like the linear Stern-Volmer calibrations (Fig. 4B). τ_0 for PdBP-PPS was 397.0±1.1 (similar to PS matrix³⁶) and τ_q was 131.0±0.7 μ s (21kPa, 20°C). Hence, PdBP-PPS sensors are about 5-6 times more sensitive than PtBP, which makes them useful for the O₂ range 0.1-21 kPa. Since the excitation and emission bands of PdBP and PtBP are shifted by only 10-30 nm (Fig. 5C), both sensor types can potentially be measured on the same instrument.

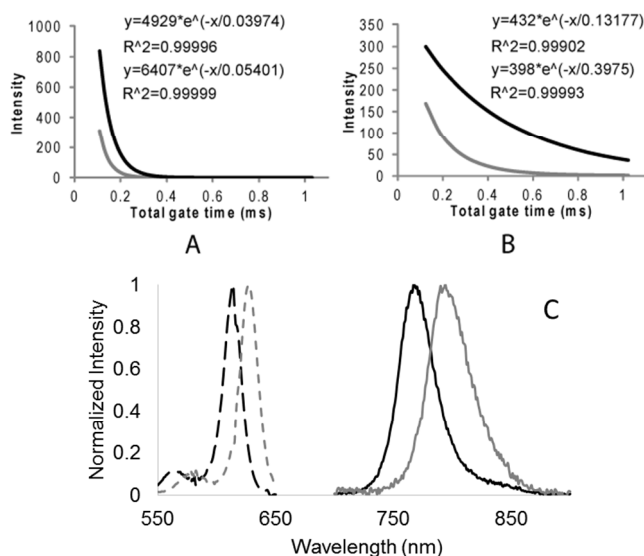


Figure 5. Phosphorescence decays of the PtBP-PPS (A) and PdBP-PPS (B) sensors at 21 kPa (grey line) and 0 kPa (black line) O₂, 20°C. Normalised excitation (dashed lines) and emission (solid lines) spectra (C) of PtBP (black) and PdBP (grey) sensors.

The lower O₂ permeability and significant thickness of PPS matrix slow down sensor response. Our 70 micron thick sensor films produced T_{95%}=11.5 min and T_{90%}=6.7min at 10°C, being similar in water and gas phase. Such response time is acceptable for many industrial applications. The response becomes shorter at higher temperatures (3min at 50°C for T_{100%}) and for thinner films (in line with the theory of O₂ diffusion in polymers).

Lateral and in-depth micro-heterogeneity of PtBP-PPS sensors was analysed by confocal fluorescence and phosphorescence lifetime imaging microscopy (PLIM). The distribution of intensity and lifetime signals for three Z-stacks from the same sensor (0, 20 and 40 μ m below the surface) is shown in Fig. 6. At higher depth surface maps show a greater variation of the lifetime, which we attribute to increased light scattering by the upper layers and more variable intensity signals received by the detector. Nonetheless, lifetime values across the film width and depth show symmetrical normal distribution. Similar was observed in spot-crazed HDPE sensors²⁵. Photostability of PPS-PtBP sensors was also examined and compared to existing O₂ sensors. After 8h of continuous illumination at maximal power of the 615 nm LED (FirestingTM instrument) in air

atmosphere at 20°C, PtBP-PPS sensors showed no photodegradation or changes in O₂ calibration whatsoever. For comparison, solvent-crazed HDPE-PtBP sensor showed a 6% decrease in intensity signal and a significant downward drift of the phase signal (0.248 degrees). These results reflect the high stability of O₂ sensors derived from PPS, with respect to photodegradation of the indicator dye (intensity signal) and the polymer (lifetime or K_{s-v}). This is consistent with the recent study in which major influence of the polymer matrix on operational performance of O₂ sensors was demonstrated.³⁷

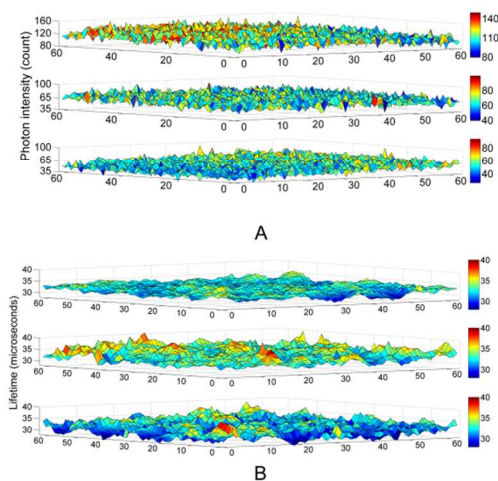


Figure 6. Phosphorescence intensity (A) and lifetime (B) images of the PPS sensors produced by high-resolution confocal microscopy. 2D surface plots are shown for the regions (64x64 pixels, 366 μ m²) located at the surface (top), 20 μ m (centre) and 40 μ m (bottom) deep.

The spot-crazed PtBP-PPS sensors were stable at temperatures 10-50°C (the range of highest practical importance): after continuous use for 1 week at 50°C no detectable changes in O₂ calibration were observed. However, steam sterilisation (autoclaving at 121°C for 45 min) or baking for 1-2h in a dry oven at 150 and 200°C significantly increased their lifetime values and induced a step-change in O₂ calibration. We link these effects to phase transitions in PPS (T_g = 91.2°C), which alter the nanoporous structure and microenvironment of dye molecules. Nonetheless, PPS sensors can be sterilized by γ -radiation, ethylene oxide or hydrogen peroxide³⁸⁻³⁹, which makes them usable in packaging, medical and food applications. According to the US FDA Food Contact Notification (FCN) 1083, PPS production polymers may be used as components in the manufacture of food-contact articles for repeat-use food-contact applications⁴⁰.

Conclusions

Discrete optical oxygen sensors based on extruded PPS films and PtBP and PdBP phosphorescent dyes were produced by spot-crazing in 2-butanone. The new polymer and easy to control and bio-sustainable fabrication technology yielded the

composite materials with useful operational characteristics and advantages over the existing O₂ sensors. The sensors possess linear Stern-Volmer calibrations and temperature trends over the O₂ range 0-100 kPa, high spatial and in-depth homogeneity, robustness and reproducibility, and negligible effect of humidity. These features make them promising for large scale applications such as packaging.

Acknowledgements

Financial support of this work by the Irish Department of Agriculture, Food and Marine, grant DAFM/11/F/015, and by the Russian Foundation for Basic Research, project No 14-03-00617a is gratefully acknowledged. Authors wish to thank Dr. R. Dmitriev and Mr. J. Jenkins for the help in imaging experiments, and Dr. S.B. Zezin for the WAXS measurements and helpful discussion.

Notes and references

^a Biochemistry Department, Cavanagh Pharmacy Building, University College Cork, Cork, Ireland.

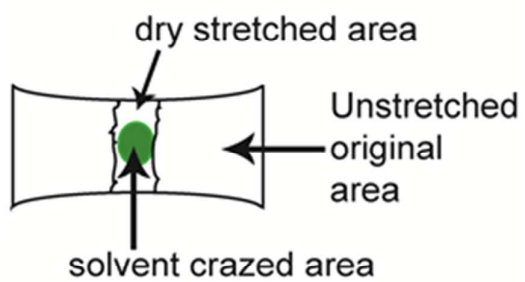
^b Department of Polymer Chemistry, Moscow State University, Leninskie Gory, Moscow, Russian Federation.

^c Department of Food Science and Nutrition, University College Cork, Cork, Ireland.

* E-mail: d.papkovsky@ucc.ie

- Mills, A., Oxygen indicators and intelligent inks for packaging food. *Chem Soc Rev* **2005**, *34* (12), 1003-1011.
- Ruggi, A.; van Leeuwen, F. W. B.; Velders, A. H., Interaction of dioxygen with the electronic excited state of Ir(III) and Ru(II) complexes: Principles and biomedical applications. *Coord Chem Rev* **2011**, *255* (21-22), 2542-2554.
- Quaranta, M.; Borisov, S. M.; Klimant, I., Indicators for optical oxygen sensors. *Bioanal Rev* **2012**, *4* (2-4), 115-157.
- Papkovsky, D. B.; Dmitriev, R. I., Biological detection by optical oxygen sensing. *Chem Soc Rev* **2013**.
- Klimant, I.; Kuhl, M.; Glud, R. N.; Holst, G., Optical measurement of oxygen and temperature in microscale: strategies and biological applications. *Sensor Actuators B-Chem* **1997**, *38* (1-3), 29-37.
- Amao, Y.; Okura, I., Optical oxygen sensor devices using metalloporphyrins. *J Porphyrins Phthalocyanines* **2009**, *13* (11), 1111-1122.
- Amao, Y., Probes and polymers for optical sensing of oxygen. *Microchim Acta* **2003**, *143* (1), 1-12.
- Kamachi, T.; Okura, I., 56 Application of Porphyrins and Related Compounds as Optical Oxygen Sensors. In *Handbook of Porphyrin Science*, 2010, pp 297-348.
- Tian, Y.; Shumway, B. R.; Meldrum, D. R., A New Cross-Linkable Oxygen Sensor Covalently Bonded into Poly(2-hydroxyethyl methacrylate)-co-Polyacrylamide Thin Film for Dissolved Oxygen Sensing. *Chem Mater* **2010**, *22* (6), 2069-2078.
- Papkovsky, D. B.; Ovchinnikov, A. N.; Ogurtsov, V. I.; Ponomarev, G. V.; Korpela, T., Biosensors on the basis of luminescent oxygen sensor: the use of microporous light-scattering support materials. *Sensor Actuators B-Chem* **1998**, *51* (1-3), 137-145.
- Koren, K.; Borisov, S. M.; Saf, R.; Klimant, I., Strongly Phosphorescent Iridium(III)-Porphyrins - New Oxygen Indicators with Tuneable Photophysical Properties and Functionalities. *Eur J Inorg Chem* **2011** (10), 1531-1534.
- von Bultzingslowen, C.; McEvoy, A. K.; McDonagh, C.; MacCraith, B. D.; Klimant, I.; Krause, C.; Wolfbeis, O. S., Sol-gel based optical carbon dioxide sensor employing dual luminophore referencing for application in food packaging technology. *Analyst* **2002**, *127* (11), 1478-1483.
- Li, X. G.; Huang, M. R.; Bai, H., High-resolution thermogravimetry of poly(phenylene sulfide) film under four atmospheres. *J Appl Polymer Sci* **2002**, *83* (9), 1940-1946.
- McKeen, L. W., *Permeability Properties of Plastics and Elastomers*. Elsevier Science: **2011**.
- Osborn D. J. III, B. G. L., Ghosh Ruby N., Mo6C112-Incorporated Sol-Gel for Oxygen Sensing Applications. *J Sol-Gel Sci Technol* **2005**, *36* (1), 5-10.
- Basu BJ, K. J., Studies on the oxygen sensitivity and microstructure of sol-gel based organic-inorganic hybrid coatings doped with platinum porphyrin dye. *J Sol-Gel Sci Technol*, **2009**, *52* (1), 24-30.
- Volynskii, A. L.; Nikonorova, N. I.; Volkov, A. V.; Moskvina, M. A.; Tunyan, A. A.; Yaryshev, N. G.; Arzhakova, O. V.; Dolgova, A. A.; Rukhlya, E. G.; Trofimchuk, E. S.; Abramchuk, S. S.; Yarysheva, L. M.; Bakeev, N. F., Preparation method for noble metal-polymer matrix nanocomposites. *Colloid J* **2010**, *72* (4), 464-470.
- Volynskii, A. L.; Bakeev, N. F., A new approach to the preparation of nanocomposites based on a polymer matrix. *Polymer Science Series C* **2011**, *53* (1), 35-47.
- Volkov, A. V.; Polyanskaya, V. V.; Moskvina, M. A.; Tunyan, A. A.; Zezin, S. B.; Dement'ev, A. I.; Volynskii, A. L.; Bakeev, N. F., The structure of polypropylene-TiO₂ organo-inorganic nanocomposites prepared via solvent crazing. *Colloid J* **2013**, *75* (1), 40-48.
- Rukhlya, E. G.; Litmanovich, E. A.; Dolinnyi, A. I.; Yarysheva, L. M.; Volynskii, A. L.; Bakeev, N. F., Penetration of Poly(ethylene oxide) into the Nanoporous Structure of the Solvent-Crazed Poly(ethylene terephthalate) Films. *Macromolecules* **2011**, *44* (13), 5262-5267.
- Toncelli, C.; Arzhakova, O. V.; Dolgova, A.; Volynskii, A. L.; Bakeev, N. F.; Kerry, J. P.; Papkovsky, D. B., Discrete phosphorescent oxygen sensors produced from high density polyethylene films by local solvent-crazing. *Anal Chem* **2014**, *86*(3), 1917-1923.
- Becker, W.; Bergmann, A.; Biskup, C., Multispectral fluorescence lifetime imaging by TCSPC. *Microsc Res Tech* **2007**, *70* (5), 403-409.
- Haugland, R. P.; Spence, M. T. Z.; Johnson, I. D., *The Handbook: A Guide to Fluorescent Probes and Labeling Technologies*. Molecular Probes: **2005**.
- Borchert, N.; Hempel, A.; Walsh, H.; Kerry, J. P.; Papkovsky, D. B., High throughput quality and safety assessment of packaged green produce using two optical oxygen sensor based systems. *Food Control* **2012**, *28* (1), 87-93.

25. Toncelli, C.; Arzhakova, O. V.; Dolgova, A.; Volynskii, A. L.; Bakeev, N. F.; Kerry, J. P.; Papkovsky, D. B., Oxygen-Sensitive Phosphorescent Nanomaterials Produced from High-Density Polyethylene Films by Local Solvent-Crazing. *Anal Chem* **2014**, *86* (3), 1917-1923.
26. Wilhelm, S.; Wolfbeis, O. S., Irreversible sensing of oxygen ingress. *Sensor Actuators B-Chem* **2011**, *153* (1), 199-204.
27. Brady, D. G., The crystallinity of poly(phenylene sulfide) and its effect on polymer properties. *J Appl Polym Sci* **1976**, *20* (9), 2541-2551.
28. Seo, K. H.; Park, L. S.; Baek, J. B.; Brostow, W., Thermal behaviour of poly (phenylene sulfide) and its derivatives. *Polymer* **1993**, *34* (12), 2524-2527.
29. Hill Jr., H. W. In: High Performance Polymers and Composites. *Kroschwitz, J. I. Ed., 1991, John Wiley & Sons: New York*, pp 551-577.
30. CETEX, PPS Guide Lines; Ten Cate Advanced Composites. *Nijverdal, Netherlands* **2003**, 32.
31. Mo, Z.; Zhang, H., The Degree of Crystallinity in Polymers by Wide-Angle X-Ray Diffraction (Waxd). *J Macromol Sci, Part C* **1995**, *35* (4), 555-580.
32. Volynskii, A. L.; Bakeev, N. F., *Solvent Crazing of Polymers*. Elsevier Science: **1995**.
33. Badocco, D.; Mondin, A.; Pastore, P., Determination of thermodynamic parameters from light intensity signals obtained from oxygen optical sensors. *Sensor Actuators B-Chem* **2012**, *163* (1), 165-170.
34. Borisov, S. M.; Nuss, G.; Haas, W.; Saf, R.; Schmuck, M.; Klimant, I., New NIR-emitting complexes of platinum(II) and palladium(II) with fluorinated benzoporphyrins. *J Photochem Photobiol A-Chem* **2009**, *201* (2-3), 128-135.
35. Eaton, K.; Douglas, P., Effect of humidity on the response characteristics of luminescent PtOEP thin film optical oxygen sensors. *Sensor Actuators B-Chem* **2002**, *82* (1), 94-104.
36. Borisov, S. M.; Papkovsky, D. B.; Ponomarev, G. V.; DeToma, A. S.; Saf, R.; Klimant, I., Photophysical properties of the new phosphorescent platinum(II) and palladium(II) complexes of benzoporphyrins and chlorins. *J Photochem Photobiol A-Chem* **2009**, *206* (1), 87-92.
37. Enko, B.; Borisov, S. M.; Regensburger, J.; Baumler, W.; Gescheidt, G.; Klimant, I., Singlet oxygen-induced photodegradation of the polymers and dyes in optical sensing materials and the effect of stabilizers on these processes. *J Phys Chem A* **2013**, *117* (36), 8873-82.
38. Massey, L. K., *The Effect of Sterilization Methods on Plastics and Elastomers, 2nd Edition*, . Technology & Engineering: **2004**, p.413.
39. Zajko, S.; Klimant, I., The effects of different sterilization procedures on the optical polymer oxygen sensors. *Sensor Actuators B-Chem* **2013**, *177*, 86-93.
40. US Food and Drug Administration, Food Contact Notification (FCN) 1083.



Phosphorescent oxygen sensors produced by localised solvent-crazing of polyphenylene sulphide films are described.